

Vortex creation during magnetic trap manipulations of spinor Bose-Einstein condensates

A.P. Itin,^{1,2} T. Morishita,¹ M. Satoh,¹ O.I. Tolstikhin,³ and S. Watanabe¹

¹*Department of Applied Physics and Chemistry,
University of Electro-Communications,
1-5-1, Chofu-ga-oka, Chofu-shi, Tokyo 182-8585, Japan*

²*Space Research Institute, RAS, Moscow, Russia*

³*Russian Research Center “Kurchatov Institute”,
Kurchatov Square 1, Moscow 123182, Russia*

We investigate several mechanisms of vortex creation during splitting of a spinor BEC in a magnetic trap controlled by a pair of current carrying wires and bias magnetic fields. Our study is motivated by a recent MIT experiment on splitting BECs with a similar trap, where unexpected fork-like structure appeared in the interference fringes corresponding to interference of two condensates, one with and the other without a singly quantized vortex. It is well-known that in a spin-1 BEC in a quadrupole trap a doubly quantized vortex is produced topologically by a “slow” reversal of bias magnetic field B_z . We find that in the magnetic trap considered it is also possible to produce a 4- and 1-quantized vortex in a spin-1 BEC. The latter is possible, for example, during the magnetic field switching-off process. We therefore provide a possible explanation for the unexpected interference patterns in the experiment. We also give an example of the creation of singly quantized vortices due to “fast” splitting, which is a possible alternative mechanism of the interference pattern.

I. INTRODUCTION

Coherent manipulation of matter-waves is presently a very important experimental and theoretical field. Coherent splitting of matter waves into spatially separate atomic wave packets with a well-defined relative phase is necessary for atom interferometry and quantum information processing applications. Bose-Einstein condensates (BECs) open new unprecedented perspectives in this direction. Coherent splitting of a BEC was recently realized both in an optical double-well trap [1] and in a magnetic chip-based double-well trap [2]. In the latter experiment, the magnetic trap was produced by a pair of current carrying wires and a bias field used to control the distance between the wells [3]. An intriguing feature of this experiment was appearance of a fork-like structure in the absorption image of interference fringes designating creation of a singly quantized vortex in one of the wells. Thus perturbations during condensate manipulations were violent enough to generate vortices. To identify possible mechanisms of vortex creation is an inevitable challenge for future pursuit of BEC interferometry with such kind of an experimental configuration.

Here we study two independent scenarios that could lead to vortex creation. One of them is the phase imprinting during the switching-off process (due to different decay times of the bias fields and the fields of the two wires), while the other is dynamical vortex creation during fast splitting. Although the switching-off time in the particular experiment [2] was only about $20 \mu s$ (a duration much shorter than the inverse of any trap frequency), it is slow as compared to the Larmor frequency in the magnetic field of order of 1G. Therefore, adiabatic imprinting might take place. On the other hand, the authors of Ref. [2] think the phase imprinting mechanism is an unlikely explanation for the vortex creation since they have never observed interference pattern of a doubly quantized vortex (which is created topologically in spin-1 condensates when zero point of the magnetic field crosses through condensates). We find realistic scenarios for a singly quantized vortex interference pattern to appear as a result of topological phase imprinting during the switching-off process. Indeed as we assume exponential decay of magnetic fields produced by the two wires and the bias field B_z with different decay constants, with parameters close to the experiment we obtain numerically that a large part of the atoms (about half of the condensate) can be transferred to the component Ψ_0 (i.e., with $m = 0$ in z -quantized basis, see Eqs. (1) and (2) for notation) which has singly quantized vortices around each of the two minima of the

magnetic field. In contrast, when we try to obtain doubly quantized vortices using bias field B_z reversal, it turns out to be more difficult. At such short timescales, only a small part of the population is transferred to the component Ψ_1 with doubly quantized vortices, while the rest of the population is redistributed among other components. Creation of doubly quantized vortices in such a configuration requires times of the order of hundreds of μs . We also present an example of dynamical vortex creation during fast splitting. In this case, the condensate (including the Ψ_{-1} component) acquires winding phase during the splitting process. This leads to clear fork-like structures in all components and thus the total density upon expansion. Although in our calculations this requires a sufficiently shorter time of splitting than that which was actually effected in the real experiment [2], it might be caused by the oversimplified model (without jitter or fluctuations of the magnetic field, etc).

The rest of the paper is organized as follows. In Sec. II we introduce the model (spinor BEC described by 2D GP equation with spin degrees of freedom), describe the configuration of the magnetic field given by the two-wires setup, and its weak- and strong-field seeking states. In Sec. III, we present numerical results on vortex creation in the system. In Sec. IIIA we study several examples of how an unexpected topological phase imprinting could have taken place in the MIT experiment. There we take into account gravity and use realistic parameters relevant to the experiment. We assume that after switching off the magnetic field the B_z field decays faster than transversal magnetic field B_\perp , which can lead to the phase imprinting. In Sec. IIIB we present examples of dynamical vortex creation during splitting process. When split slowly in 30 ms, the condensate develops no vortex. However, reduction of the splitting duration to about 5 ms, vortices are created. Then, even in the case where the switching-off process leaves all population in the initial Ψ_{-1} component, expansion of condensates produces very clear forks in the interference pattern.

II. THE MODEL

A. Spinor Bose condensate

We consider a BEC of alkali atoms with hyperfine spin $F = 1$ using the z -quantized basis [4]. The order parameter is expanded as

$$\Psi = \sum_{m=\pm 1,0} \Psi_m |m\rangle, \quad (1)$$

where $|m\rangle$ are eigenvectors of F_z :

$$|1\rangle = (1, 0, 0)^T, \quad |0\rangle = (0, 1, 0)^T, \quad |-1\rangle = (0, 0, 1)^T. \quad (2)$$

We use the time-dependent form of the GP equation with spin degrees of freedom developed in [4]:

$$i\frac{\partial}{\partial t}\Psi_j = \left[-\frac{\hbar^2}{2M}\nabla^2 + g_n \sum_l |\Psi_l|^2 + V(\mathbf{r})\right]\Psi_j + \left[g_s \sum_\alpha \sum_{lp} (\Psi_l(F_\alpha)_{lp}\Psi_p)(F_\alpha)_{jk} - \mathcal{B}_{jk}\right]\Psi_k, \quad (3)$$

$$\mathcal{B}_{jk} = \begin{pmatrix} B_z & \frac{B_x - B_y}{\sqrt{2}} & 0 \\ \frac{B_x + B_y}{\sqrt{2}} & 0 & \frac{B_x - B_y}{\sqrt{2}} \\ 0 & \frac{B_x + B_y}{\sqrt{2}} & -B_z \end{pmatrix}$$

where F_α ($\alpha = x, y, z$) are the angular momentum operators in the basis of the eigenvectors of F_z :

$$F_x = \frac{1}{\sqrt{2}} \begin{pmatrix} 0 & 1 & 0 \\ 1 & 0 & 1 \\ 0 & 1 & 0 \end{pmatrix}, \quad F_y = \frac{i}{\sqrt{2}} \begin{pmatrix} 0 & -1 & 0 \\ 1 & 0 & -1 \\ 0 & 1 & 0 \end{pmatrix}, \quad F_z = \frac{1}{\sqrt{2}} \begin{pmatrix} 1 & 0 & 0 \\ 0 & 0 & 0 \\ 0 & 0 & -1 \end{pmatrix},$$

and $g_n = 4\pi\hbar^2(a_0 + 2a_2)/3m$ is the spin-independent and $g_s = 4\pi\hbar^2(a_2 - a_0)/3m$ is the spin-dependent interaction coefficients. Here the scattering lengths a_0 and a_2 characterize collisions between atoms with total spin 0 and 2, m is the atomic mass.

We consider a condensate of ^{23}Na , which was used in the experiment of [2]. Parameters of Na are $M = 3.81 \cdot 10^{-26}$ kg, $a_2 = 2.75\text{nm}$, $a_0 = 2.46\text{nm}$ [6]. Spin-independent potential $V(\mathbf{r})$ is provided either by gravity as in the MIT experiment ($V(\mathbf{r}) = -Mgy$, we consider this case in Section 3), or, in principle, ‘‘optical plug’’ can be used. We assume the wavefunction of either component does not depend on the z coordinate, i.e. the condensate is quasi-2D. We therefore use two-dimensional nonlinearity parameters g_n^{2D} and g_s^{2D} which are related as $g_n^{2D}/g_s^{2D} = 27.44$. Configuration of the magnetic field is described in the next subsection.

B. The magnetic trap

We use a two-wires setup suggested in Ref. [3]. It was used in a recent experiment of Y. Shin *et al.* [2], where several important elements were added making the system

essentially three-dimensional. We consider a two-dimensional trap here to simplify numerical calculations. Magnetic field produced by two parallel current-carrying wires is given by

$$\begin{aligned} B_x^W &= \frac{-y}{(x+d)^2+y^2} + \frac{-y}{(d-x)^2+y^2}, \\ B_y^W &= \frac{x+d}{(x+d)^2+y^2} + \frac{-d+x}{(d-x)^2+y^2}, \end{aligned} \quad (4)$$

where $2d$ is the distance between the wires.

Additional magnetic field B_z is added along z direction, and bias field B_x^B is added in x direction: $B_x = B_x^W + B_x^B$. For weak-field-seeking atoms, amplitude of magnetic field $B(x, y)$ plays the role of trapping potential (while the potential for strong field-seeking atoms is $-B(x, y)$). At certain critical $B_x^B = B_{x_0}$ the trap potential $B(x, y)$ has a single minimum located on distance d away from the surface, at the middle of the two wires. At B_x^B greater or smaller than B_{x_0} the potential has two wells: when $\Delta B_x \equiv B_x^B - B_{x_0} > 0$, the two wells are separated in the x direction, while for $\Delta B_x < 0$ they are separated in the y direction and has equal x -coordinates of their centers. Addition of bias magnetic field B_y^B along the y -axis rotates these two wells in the xy plane. It is important that the critical single well potential is harmonic (corresponding to hexapole configuration of magnetic field), while either of the separated double wells is quadrupole. We assume uniform B_z is applied to the system. In numerical calculations, we used the parameters close to the experiment of Ref. [2]: $d = 150\mu\text{m}$ (this corresponds to the distance between the wires of $300\mu\text{m}$), $B_{x_0} = 24\text{G}$, $B_z(0) = 1\text{G}$.

C. Strong- and weak-field seeking states in two-wires trap

The important feature of static magnetic traps is that it confine the weak-field seeking state(s) (WFSS) which has a higher energy than the strong-field seeking state(s) (SFSS). Therefore, there is some difficulty in numerical preparation of initial states, since straightforward imaginary time propagation would lead to SFSS. One need to search for a solution using a WFSS ansatz which is derived from the eigenvector of the \mathcal{B} matrix. The eigenvalues of \mathcal{B} are $\pm B$ (where $B = \sqrt{B_x^2 + B_y^2 + B_z^2}$) and 0 (the latter corresponding to the neutral field-seeking state, NFSS), and the eigenvector corresponding to WFSS is

$$|-1\rangle = \frac{1}{2B} \begin{pmatrix} (B - B_z)(B_x - iB_y)/B_\perp \\ -\sqrt{2}B_\perp \\ (B + B_z)(B_x + iB_y)/B_\perp \end{pmatrix} \quad (5)$$

Suppose we have configuration with $\Delta B_x = 0$ (so the wells are coalesced in a single harmonic well). When $(B_x \pm iB_y)/B_\perp = e^{\mp 2i\phi}$ in the vicinity of the minimum of the well, where ϕ is the polar angle around the point of the minimum. The weak-field-seeking state order parameter has the form

$$\begin{pmatrix} \Psi_1 \\ \Psi_0 \\ \Psi_{-1} \end{pmatrix} = \frac{1}{2B} \begin{pmatrix} (B - B_z)(B_x - iB_y)/B_\perp \\ -\sqrt{2}B_\perp \\ (B + B_z)(B_x + iB_y)/B_\perp \end{pmatrix} \psi e^{iw\phi} = \frac{1}{2B} \begin{pmatrix} (B - B_z)e^{2i\phi} \\ -\sqrt{2}B_\perp \\ (B + B_z)e^{-2i\phi} \end{pmatrix} \psi e^{iw\phi}, \quad (6)$$

where ψ is the amplitude (common for all three components). At large B_z , almost all population is in Ψ_{-1} component. In order to avoid vorticity in this component, we should choose $w = 2$. Substituting ansatz (6) into GP equation, one obtains the one-component equation for the amplitude ψ which can be solved using imaginary time propagation to find a ground state. However, it is also possible to propagate the original three-component GP equation in the imaginary time, restricting the solution to the ansatz (6). We used both algorithms in our calculations.

One can see that one obtains a vortex with vorticity 4 from the initial non-vortex state in the critical hexapole trap by reversal of B_z . When $\Delta B_x \neq 0$, we have two quadrupole traps. In that case reversal of B_z leads to doubly quantized vortices in either trap, as was studied in several works recently (for example, Ref. [4]). It is important that the component Ψ_0 in that case contains singly quantized vortices.

III. VORTEX CREATION DURING REALISTIC MAGNETIC TRAP MANIPULATIONS

A. Phase imprinting

Bias fields B_z and B_x^B and the two-wires magnetic field B^W are created by different sources. During a switching-off process, they can behave differently. Examples of nontrivial consequences of nonsynchronous decreasing processes of magnetic fields in other situations

were considered in Refs. [7, 8]. In order to achieve topological imprinting, we consider here the switching-off process with B_z decaying faster than B_\perp (in our model calculations, we assume the fields B_x^B and B_\perp^W decay synchronously, while the field B_z decays faster). We found a time of the order of tens of μs is enough to transfer a large part of the atoms to component Ψ_0 with singly quantized vortices in each well.

In contrast, we found that in order for B_z reversal to produce considerable population of Ψ_1 component with doubly quantized vortices, much longer times are required, i.e. hundreds of μs . In the experiment of Ref. [2] switching-off time was $T_{off} \approx 20\mu\text{s}$. Larmor frequency at $B = 1\text{G}$ is ≈ 700 kHz corresponding to $\tau_L = 1.4\mu\text{s}$. Therefore, despite very short switching-off time, "adiabatic" phase imprinting still might take place. We checked this guess numerically.

Four stages of the process were carefully examined: preparation of initial state, splitting, switching-off process, and the free expansion. Firstly, we prepare the initial state in the single (critical) harmonic well using imaginary time propagation, as described in the previous Section. (In the real experiment, the condensate was prepared initially at $\Delta B_x = -140\text{mG}$ in the bottom well of the double-well potential, but it is not important for our present purpose). When, the condensate was split by ramping ΔB_x from 0 to 100 mG in real time. During this stage, almost all the population is in Ψ_{-1} component, because the B_z field of 1G is large as compared with magnetic field B_\perp in the vicinity of the minima of magnetic field, where the condensate resides. Provided the splitting is slow, Ψ_{-1} component remains without vortices (however, at fast splitting it acquires phase winding, this case is considered in the next subsection). During the third stage, the magnetic field was turned off. Faster decay of B_z may lead to creation of two singly quantized vortices in component Ψ_0 in either of the two wells. This would result in two fork-like structures in the interference pattern of this component (only one of the forks points up, because charges of the topological vortices in either well are the same (positive)). The interference fringes were formed during the fourth stage of numerical calculations: expansion of the two condensates without magnetic field. For numerical purposes, we also turned off the gravity field in the fourth stage, but we suppose this does not influence results significantly. In the real experiment, typical time of expansion was about 22 ms. In our calculations, we typically calculate up to 4 ms only.

In Fig.1, fast splitting of the condensate is shown. The condensate was prepared in the merged well (at $\Delta B_x = 0$). Splitting was done approximately in 5 ms, much faster than in

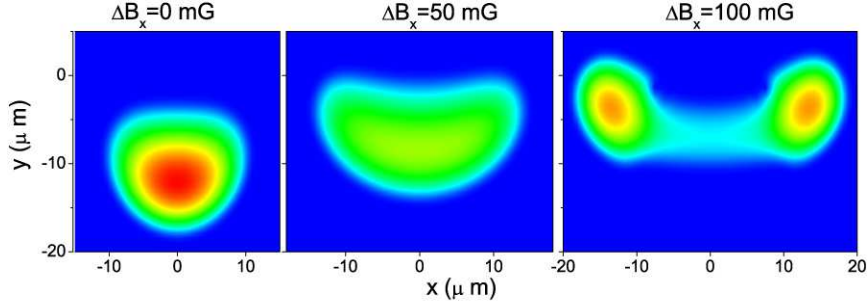


FIG. 1: Splitting of the condensate by ramping ΔB_x from 0 to 100 mG. Total density is shown. The origin of the coordinates is the merge point without gravity. Parameters are close to the experiment of Shin *et. al*; splitting was fast: time of splitting about 5ms.

the experiment. In Fig.2, slow splitting of the condensate is monitored (time of splitting about 30 ms). The final state is slightly different about 2 % of the initial population was lost because during very slow splitting. The atoms that make transitions from WFSS to SFSS fly away (they fly up towards the wires and are removed by absorbing potential on the boundaries of the mesh). The atoms that make transitions to NFSS, fly down because of the gravity (and are also removed).

Densities and phases of the components of the split condensate are presented. Component Ψ_{-1} has no vorticity, while Ψ_0 has singly quantized vortices in both wells and Ψ_1 has doubly quantized vortices. Since $B_z = 1G$, almost all population is in Ψ_{-1} component without vorticity.

In Fig. 3, interference fringes formed during expansion of the condensates are shown. Magnetic fields were switched off in approximately $20\mu s$ in such a way that no transition from Ψ_{-1} component occurred (B_z was decreased more slowly than B_{\perp}).

Then, we consider a case where B_z is decreasing faster than B_{\perp} . In Fig.4, the process of topological vortex formation is shown during switching-off process. Magnetic fields were decreasing exponentially, with B_z decaying faster, and were turned off completely at $t = 0.06\tau \approx 20\mu s$ ($\tau \approx 350\mu s$ is the characteristic time period used in the program). About half of the total population were transferred to the component Ψ_0 . An important feature of nonadiabatic transitions during process of switching-off can be noticed. The part of condensate in component Ψ_{-1} residing far from the minima of the magnetic field is more easily converted to other components than the part near the minima. As a result, decreasing

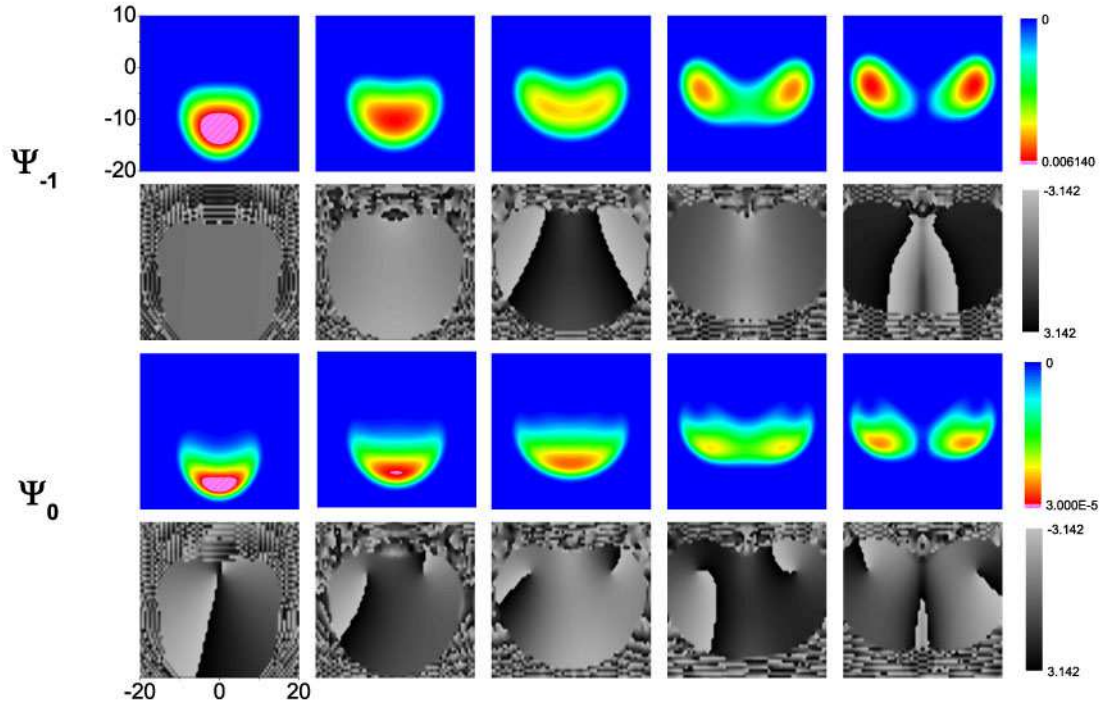


FIG. 2: Slow splitting of the condensate by ramping ΔB_x from 0 to 100 mG. Time of splitting about 30ms. For each component, density and phase profiles are depicted. In the component Ψ_0 , singly quantized vortices of topological nature are seen. Their phase singularities reside in the minima of the magnetic field which slowly move as ΔB_x is increased.

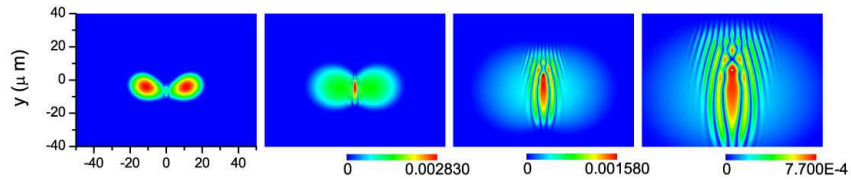


FIG. 3: Formation of fringes during expansion of the slowly split condensates. Switching-off of magnetic fields was done in such a way that almost all population (more than 99%) remains in Ψ_{-1} component.

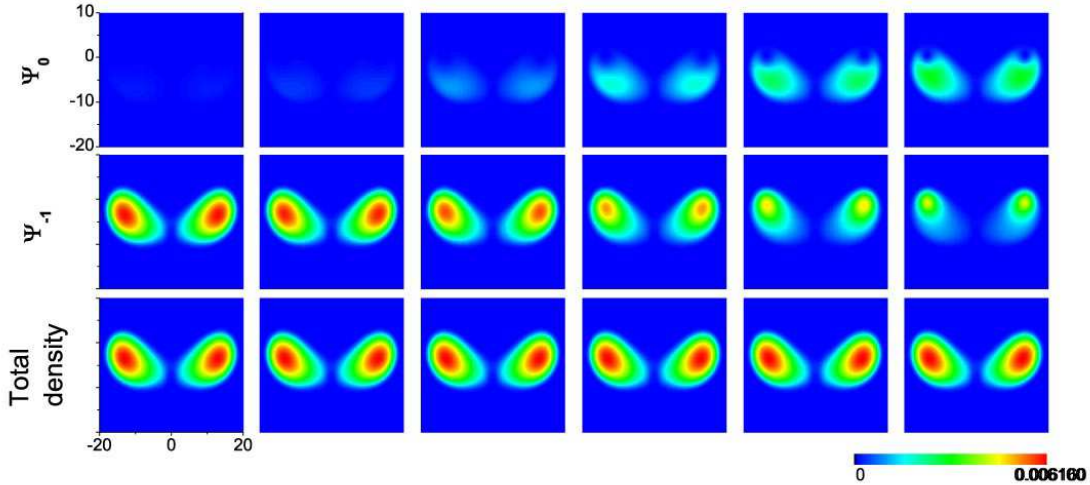


FIG. 4: Formation of singly quantized vortices in Ψ_0 component during switching-off process. B_z decay faster than B_\perp . Time of switching-off process is about $20 \mu\text{s}$.

B_z slices out a part of the condensate around the minima of the magnetic field and leaves it in the initial Ψ_{-1} component. This is due to the fact that in the region where B_\perp is not zero, a nonvanishing gap between WFSS and NFSS remains; besides, the stronger the field B_\perp is, the more slowly the total magnetic field rotates, making it easier for the spin of an atom to follow it. Quantitatively, nonadiabatic transitions due to nonsynchronously decreasing trapping magnetic fields (in other configurations) were considered recently in Ref. [7] by generalizing the Landau-Zener formula for the multilevel case. It can be seen also that during fast switching-off process, the total density is almost unaffected, therefore the nonlinear interaction coefficient g_n plays no role in the process.

Time evolution of populations of the components is shown in Fig. 5. In Fig. 6, interference fringes formed during expansion of the condensates are shown. Fork-like structure is seen in the component Ψ_0 .

Topological vortices in component Ψ_0 in both wells has equal charges. Therefore, only one fork points up (Ref. [11]). The Ψ_0 component rotates clockwise during expansion due to equal charge of the vortices, and the fork is moving up. Because of this, although during our calculations it has not appeared in total density profile, we believe that after a longer time it will show up (note that almost half of the total population is in the Ψ_0 component). The

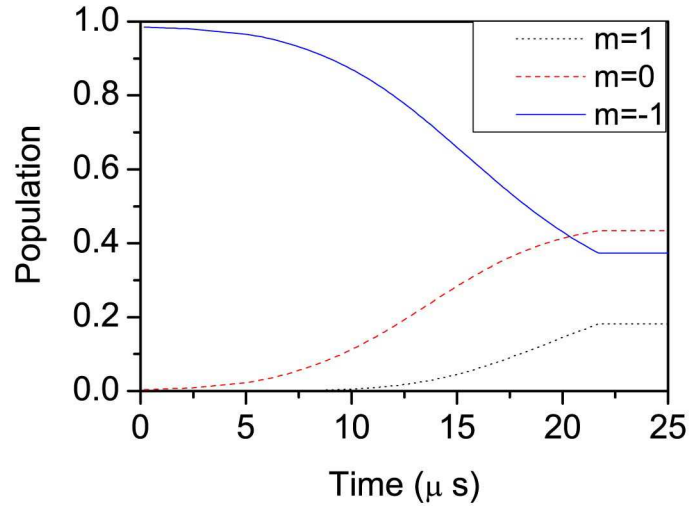


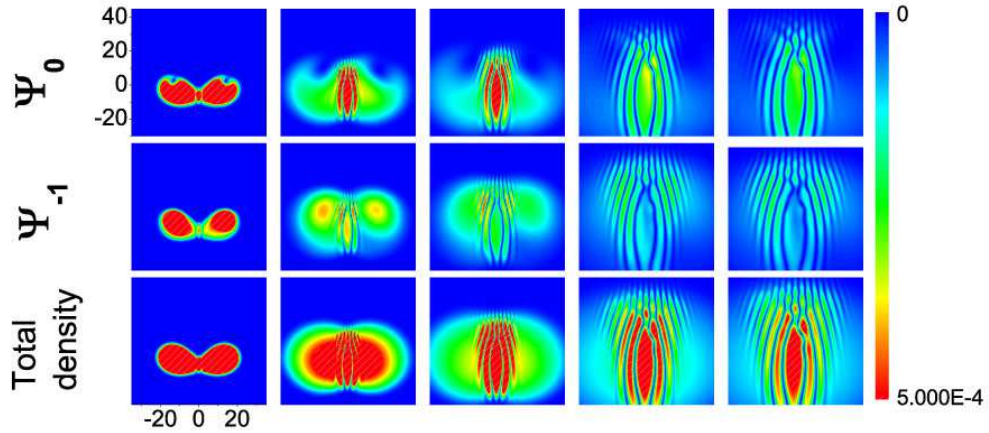
FIG. 5: Time evolution of populations of the components of the condensate during switching-off. Time of switching-off process T_{off} is about $20 \mu s$ (at this time, all remaining magnetic fields are abruptly turned off).

absence of the fork in the total density profile on early stages of expansion is related to the above-mentioned behavior of the switching-off process that leaves Ψ_{-1} component residing near the minima of magnetic field almost unaffected. After the switching-off this component therefore is concentrated at the same places where the phase singularities of component Ψ_0 are located.

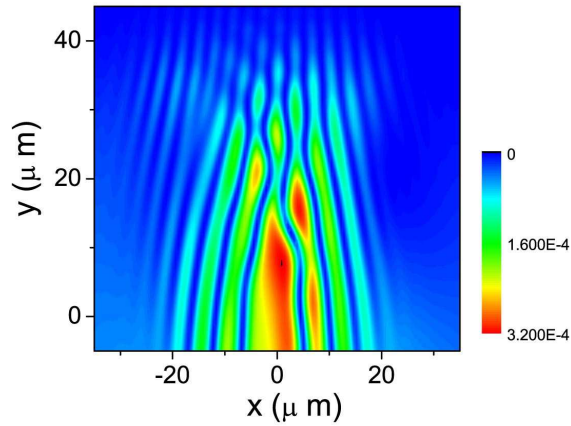
For clarity, we give also an example of vortex formation without gravity (Fig.9). Here, the both forks are clearly seen.

B. Dynamical vortex creation

In Fig.7, fast splitting of the condensate is monitored. Dynamically created vortices appear in all the components (in component Ψ_0 dynamical and topological vortices coexist). Centers of dynamically created vortices (the phase singularities) lie outside the condensate, but branch cuts go through the condensate causing phase winding across it. So this situation is different from the so-called ghost vortices appearing in studies of stirring condensates (Ref. [9]). Although vortices are almost not visible in the density profile of the condensate, its expansion leads to characteristic fork-like structures in the interference fringes due to the



(a)



(b)

FIG. 6: Formation of fringes during expansion of the condensate with imprinted vortices. Almost half of the population were transferred to the component Ψ_0 during switching-off. Topological vortices in component Ψ_0 has equal charges in both wells. Only one fork points up in the Ψ_0 component. In total density pattern, the fork have not appeared yet. However, note that in the experiment expansion took much longer time. We see that the Ψ_0 component with vortices rotates clockwise during expansion. After a long time, the fork therefore might appear in the total density pattern too (our current computational recourses forbid such a long-time propagation). (a) Density of components Ψ_0, Ψ_{-1} , and total density, (b) Density of the component Ψ_0 with the fork-like structure after approximately 4 ms of expansion.

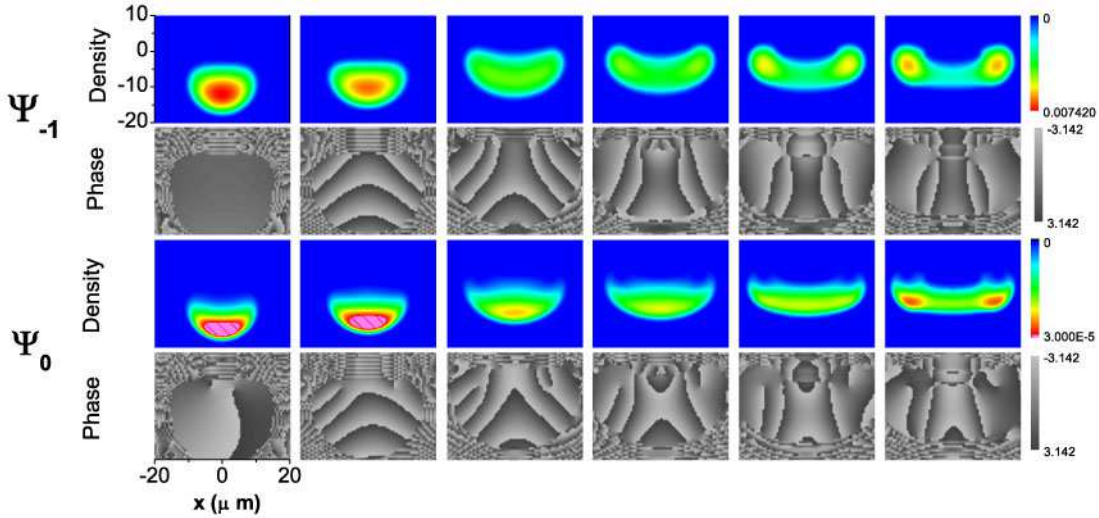
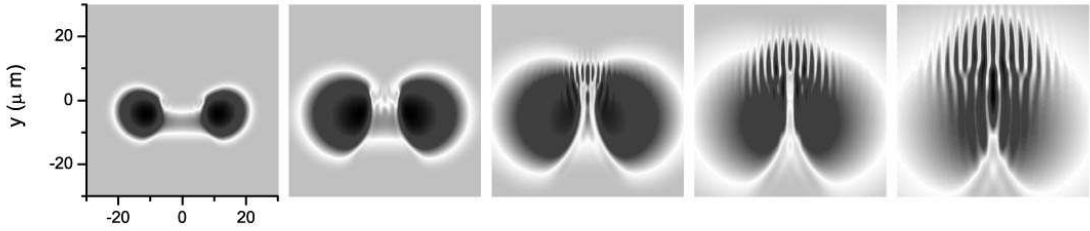


FIG. 7: Fast splitting of the condensate. Dynamical formation of vortices: vortices are formed in all components (note that more than 99% of total population is in Ψ_{-1} component). In the Ψ_0 component dynamical and topological vortices coexist. Topological vortices are the same as in Fig.2.

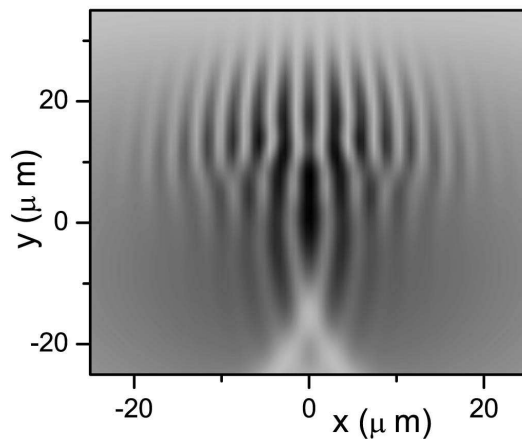
phase winding.

Magnetic field was switched off in such a way that almost no transfer to Ψ_0 occur. So, Ψ_0 component does not influence the dynamics. In Fig. 8, interference fringes resulted from the subsequent expansion are shown. Two fork-like structures (which appear in all components) are clearly seen. Vortices in the two condensates have opposite charges, therefore the forks point up (splitting of the condensate on two parts in the presence of gravity effectively causes rotation of each part in opposite directions).

To finish off, let us notice that the calculations reported were done using the sin-DVR method (with a spatial mesh of 200×160 grid points), and time propagation using the Runge-Kutta method (the method is the generalization of the one used in Ref. [10] to the case of spinor condensates). We try to model the system as close to the experimental one as possible. However, we found that, for example, g_s factor does not affect the results, i.e., the results are qualitatively the same with $g_s = 0$. The most important deviation of the model from the experimental system is its reduced dimensionality. The real system is three-dimensional, with nonuniform magnetic fields, with an additional two pairs of wires creating



(a)



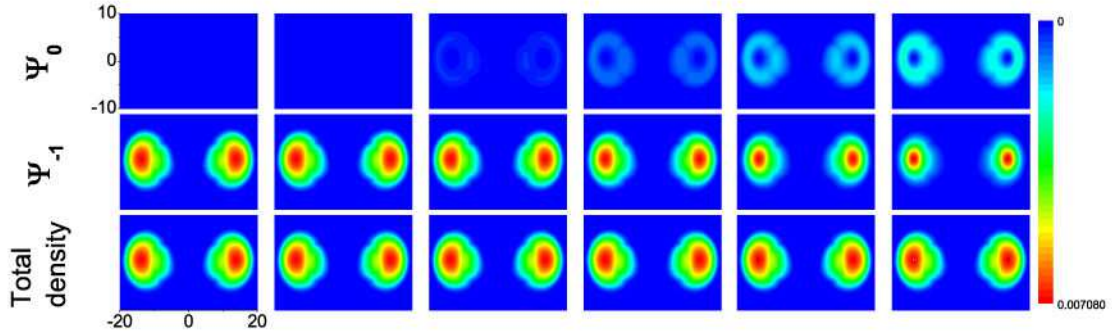
(b)

FIG. 8: Formation of fringes during expansion of the rapidly split condensates. During switching-off, almost no transfer occur to the component Ψ_0 . Dynamical vortices in the two wells have different charges, therefore the two forks point up.

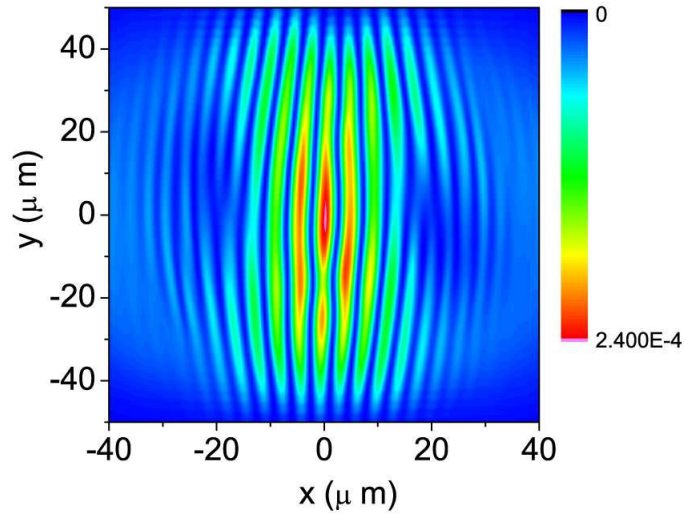
magnetic fields to compensate partly for nonuniformity of the base magnetic fields and asymmetry, etc. Such complication is presently beyond our available resources. However, we believe the study of the idealized model do allow to discuss different mechanisms of vortex creation in the experiment.

IV. CONCLUSION

The authors of the experimental work [2] supposed the phase imprinting mechanism to be unlikely for explaining the appearance of the fork-like structure and that “the observed phase singularity definitely shows the breakdown of adiabaticity”. To the contrary, we found



(a)



(b)

FIG. 9: Dynamics without gravity. (a) Formation of singly quantized vortices in Ψ_0 component during switching-off process. B_z decay faster than B_\perp . Time of switching-off process was about $20 \mu\text{s}$. (b) Fork-like structures in the density of Ψ_0 component.

a realistic scenario based on nonsynchronous decreasing processes of the magnetic fields can explain the phase singularity even within the assumption of adiabatic evolution.

However, we found that fast splitting can also lead to dynamical vortex creation, and that the dynamically created vortices produce interference patterns with the forks of better contrast. Detailed study of these processes is left for future research. In any event, the splitting of a spinor BEC is a rather violent process so that further consideration of atom interferometry with spinor BEC is necessary.

V. ACKNOWLEDGEMENTS

A.P. Itin is supported by JSPS. This work was also supported in part by Grants-in-Aid for Scientific Research No. 15540381 and 16-04315 from the Ministry of Education, Culture, Sports, Science and Technology, Japan, and also in part by the 21st Century COE program on “Coherent Optical Science”. TM was also supported in part by a financial aid from the Matsuo Foundation. We would like to acknowledge useful discussions with Prof. Y.S. Kivshar and Prof. Nakagawa.

-
- [1] Y. Shin et. al, Phys. Rev. Lett. **92**, 050405 (2004).
 - [2] Y. Shin et. al, Phys. Rev. **A 72**, 021604 (2005).
 - [3] E. A. Hinds, C. J. Vale, and M. G. Boshier, Phys. Rev. Lett. **86** , 1462 (2001).
 - [4] T. Isoshima et al., Phys. Rev. **A 61**, 063610 (2000).
 - [5] Y. Kawaguchi, M. Nakahara, and T. Ohmi, Phys. Rev. **A 70**, 043605 (2004).
 - [6] D. M. Stamper-Kurn and W. Ketterle, in Coherent Atomic Matter Waves, edited by R. Kaiser, C. Westbrook, and F. David (Springer, Heidelberg, 2001).
 - [7] P. Zhang et al., Phys. Rev. **A 73**, 013623 (2006).
 - [8] X.Q. Ma et. al, cond-mat/0509776 (2005).
 - [9] M. Tsubota, K. Kasamatsu, and M. Ueda, Phys. Rev. **A 65**, 023603 (2002).
 - [10] O.I. Tolstikhin, T. Morishita, and S. Watanabe, Phys. Rev.**A 72**, 051603(R) (2005).
 - [11] S. Inouye et. al, Phys. Rev. Lett.**87**, 080402 (2001).